Comments on Inorganic Chemistry
Publication details, including instructions for authors and subscription information:
http://www.informaworld.com/smpp/title~content=t713455155

SUPRAMOLECULAR ARSENIC COORDINATION CHEMISTRY

Timothy G. Carter[a]; W. Jake Vickaryous[a]; Virginia M. Cangelosi[a]; Darren W. Johnson[a]
[a] Department of Chemistry and Materials Science Institute, University of Oregon, Eugene, OR, USA

To cite this Article Carter, Timothy G. , Vickaryous, W. Jake , Cangelosi, Virginia M. and Johnson, Darren W.(2007) 'SUPRAMOLECULAR ARSENIC COORDINATION CHEMISTRY', Comments on Inorganic Chemistry, 28: 3, 97 — 122
To link to this Article: DOI: 10.1080/02603590701560994
URL: http://dx.doi.org/10.1080/02603590701560994

Comments on Inorganic Chemistry, 28: 97–122, 2007

ISSN: 0260-3594 print
DOI: 10.1080/02603590701560994

Taylor & Francis
Taylor & Francis Group

SUPRAMOLECULAR ARSENIC COORDINATION CHEMISTRY

TIMOTHY G. CARTER
W. JAKE VICKARYOUS
VIRGINIA M. CANGELOSI
DARREN W. JOHNSON

Department of Chemistry and Materials Science Institute, University of Oregon, Eugene, OR, USA

A flurry of research activity has emerged in recent years resulting in reliable strategies for the formation of spectacular self-assembled metal-ligand clusters and capsules. Main group ions have not shared in this burst of activity. In fact, ions in this part of the periodic table have largely been overlooked for use as directing elements in self-assembly reactions, despite the need for improved chelators for main group ions for a variety of applications. This review surveys our approach to developing design strategies to prepare self-assembled nanoscale supramolecular complexes containing main group ions, with a particular emphasis on supramolecular arsenic(III) coordination chemistry.

I. INTRODUCTION

Supramolecular Metal-Ligand Self-Assembly

Over the last decade and a half, there has been increasing interest in self-assembled nanoscale coordination complexes for use in a variety of applications including nanofabrication, molecular switches, host-guest chemistry and nanoscale chemical reactors.[1–7] The incorporation of

Address correspondence to Darren W. Johnson, Department of Chemistry and Materials Science Institute, University of Oregon, Eugene, OR 97403-1253, USA. E-mail: dwj@uoregon.edu

toxic metals and main group metalloid ions such as lead and arsenic, respectively, into self-assembled supramolecular complexes has received less scrutiny. Typically, self-assembled supramolecular complexes utilize either classic *d*-block transition metal centers with square planar, tetrahedral or octahedral coordination geometries, *f*-block metal-centers with expanded coordination geometry or, in some cases, a combination of the two.[8,9] The result is typically a high symmetry coordination complex containing metal centers with predictable coordination geometries that utilize directing ligands to assist in the self-assembly process.[10–12] Only a few examples can be found in the literature of complexes that incorporate main group elements in the self-assembly process, and of those,[13–16] only a few contain the highly toxic metalloid arsenic.[17–21] The overlying focus of our research group is to design, synthesize and study interactions between organothiol-based ligands and arsenic(III), antimony(III), lead(II) and other main group metals and metalloids as a means to improve the understanding of their coordination chemistry, specifically, and main group supramolecular chemistry as a whole.

Our supramolecular approach to metal chelation stems from the hypothesis that enhanced metal-ion specificity can be achieved by targeting the unusual coordination geometries of main group ions. Furthermore, the thermodynamic driving force provided by metal-ligand self-assembly reactions results in robust products. Typically, the self-assembly of discrete supramolecular complexes leads to high and even quantitative yields as a result of this stabilization. Additionally, other weak forces such as secondary bonding interactions further amplify the thermodynamic stability of these self-assembled nanoscale complexes.[22]

Our approach to arsenic chelation focuses on the use of rigid, multidentate organothiol ligands that target the unusual, but predictable, trigonal pyramidal coordination geometry of arsenic(III). The reversibility of As-thiolate bond formation allows for the self-assembly of discrete compounds to occur. We have successfully used this approach to synthesize dinuclear As_2L_3 assemblies and a variety of As_2L_2 macrocycles. We also review the diastereoselectivity in the self-assembly of these macrocycles and discuss the use of secondary bonding interactions as a means to bolster complex formation. We have recently reviewed the broader area of main group supramolecular chemistry;[23] this Comment details our work in supramolecular arsenic chemistry, and we offer brief

comments on recent and ongoing research in the area of supramolecular arsenic coordination chemistry in general.

Arsenic Background/Motivation

We have selected arsenic as the primary target for nanoscale coordination complex formation for three main reasons: (1) there are few chelators optimized for the preferred coordination geometry of arsenic, specifically, and the Group 15 ions in general; (2) the coordination geometry of arsenic with thiolate ligands is predictable (trigonal pyramidal); (3) As-S bonds are sufficiently labile to allow for self-assembly to occur.[24,25] Arsenic is best known for its toxicity toward humans, with the (+3) and (+5) oxidation states the most prevalent species found in the environment.[26] Arsenic occurs naturally, and is found in ores of both common and coinage metals resulting in an environmental hazard associated with mining and metal smelting.[27,28] Naturally contaminated well water has reached catastrophic proportions in Bangladesh, exposing tens of millions of people to arsenic, resulting in numerous types of cancers, skin afflictions and acute poisoning.[29–31] Locally, a survey conducted of the Willamette Basin in western Oregon, USA, concluded that more than 20 percent of wells tested have levels above the current EPA limit of 10 μg/L.[32] With the ever-expanding population growth in the Willamette Basin (and the world as a whole), the likelihood of human exposure increases greatly, thus making research geared toward the study of arsenic and other toxic ions essential.

Ligand Design Strategy for Supramolecular Arsenic Complexes

Although the (+5) oxidation state of arsenic is the most prevalent form found in surface water,[33] it is the (+3) state that is more toxic to humans as well as a more challenging target for remediation.[34] Arsenic(III) species have a high affinity for thiol containing biological structures such as cysteine residues in proteins and enzymes.[35,36] When coordinated with organothiolate ligands, As(III) typically prefers a trigonal-pyramidal geometry with a stereochemically active lone pair.[37,38] In rare instances, arsenic(III) can adopt a distorted octahedral or even tetrahedral geometry, typically the result of weakly coordinating sulfur, oxygen or nitrogen atoms located in close proximity to the arsenic thiolate center.[16,39,40]

Secondary Bonding Interactions Stabilize Supramolecular Structures

Secondary bonding interactions have the potential to assist in the formation of self-assembled complexes containing organothiol-based ligands and main group elements. SBI's can occur between main group metals and aromatic systems, heteroatoms such as O, N, S and the halogens.[22,41,42] Numerous examples are appearing in the literature where supramolecular chemists are utilizing SBI's as a design criterion to aid in the self-assembly process. In doing so, supramolecular chemists are expanding the forces that drive self-assembly reactions.[1,43]

The most comprehensive study to date of secondary bonding interactions with arsenic describes the interactions between As(III) and either thiocarboxylic or dithiocarboxylic acid ligands.[44] Utilizing crystallographic and computational data, Tani and coworkers successfully measured close-contact distances with a number of substituted arsenic complexes and neighboring thiocarboxylato or dithiocarboxylato ligands. They then compared their findings to compounds devoid of secondary bonding interactions and discovered that often, in the solid state, ligands were twisted out of plane to maximize close-contact interactions between the arsenic metal center and either the oxygen or sulfur of the carboxylate group. Additionally, bond elongation was observed suggesting that the interaction occurs between the nonbonding lone pairs of either a ligand oxygen or sulfur atom and the σ^* orbital of an As-S bond (Figure 1). In some instances, As-S bond lengthening of as much as 0.19 Å was observed, consistent with the population of an As-S σ^* orbital caused by a charge transfer from the heteroatom lone pair to the antibonding orbital of arsenic. UV/Vis spectroscopy provided confirmation

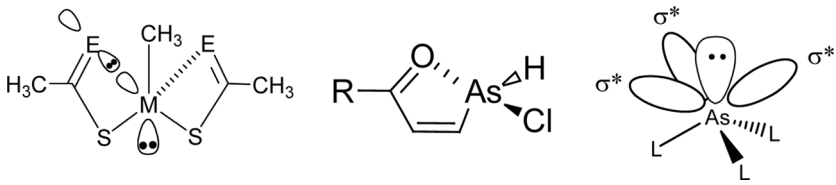

Figure 1. (left) Secondary bonding interactions between the lone pair of E (E = O or S) and an adjacent σ^* orbital of a metal center (M = As) resulting in bond elongation. (center) Model system for computational determination of As···O SBI strength. (right) Qualitative diagram depicting the approximate positions of the As-L σ^* orbitals. Each σ^*orbital is located directly opposite an As-L bond.

of this charge transfer interaction by the observation of hypsochromic, or higher energy, peak migrations.

Despite this extensive experimental work, quantification of the strength of the interaction between arsenic and the adjacent heteroatoms remains elusive. However, computational calculations of stabilization energies based on phosphorous-oxygen and phosphorous-sulfur model interactions concluded that arsenic has a higher SBI stabilization energy than phosphorous. This was demonstrated experimentally by a decrease in the measured SBI's between arsenic and the heteroatoms compared to phosphorus despite the larger atomic radius of arsenic (Figure 1).

II. SELF-ASSEMBLY OF DISCRETE DINUCLEAR ASSEMBLIES

M_2L_3 Complexes

1,4-bis(mercaptomethyl)benzene (H_2**1**, Figure 2) has the appropriate functionality and geometry to act as a bridging ligand between multiple arsenic ions. In the presence of KOH in methanol and tetrahydrofuran, 1,4-bis(mercaptomethyl)benzene (H_2**1**) and $AsCl_3$ assemble into a dinuclear As_2**1**$_3$ complex.[17] Slow diffusion of pentane into a solution of As_2**1**$_3$ in chloroform yields crystals suitable for X-ray diffraction. The solid state structure is shown in Figure 2.

In this assembly, there are several close contacts between the arsenic ions and the aromatic rings. Each arsenic ion makes close contacts with

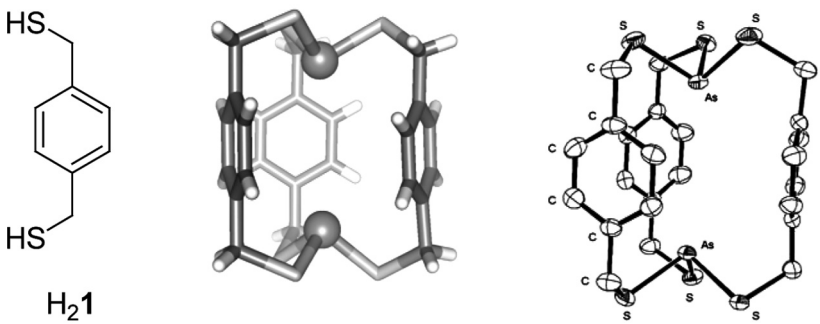

Figure 2. (left) 1,4-Bis(mercaptomethyl)benzene H_2**1**; (center) wireframe representation of the self-assembled As_2**1**$_3$ complex showing both arsenic atoms pointing into the cavity of the complex; (right) ORTEP diagram of As_2**1**$_3$. The cocrystallized $CHCl_3$ solvent is omitted for clarity.

two carbons of each aromatic ring—in effect, each arsenic ion is involved in an η^2-secondary bonding interaction with each of three aromatic rings. Off-center arsenic-arene interactions such as these have previously been observed in the packing of separate discrete molecules. For example, Schmidbaur and coworkers crystallized a cyclophane adduct of arsenic trichloride with η^1 and η^2-secondary arsenic-arene interactions.[17,45] The $As_2\mathbf{1}_3$ assembly (Figure 2) exhibits multiple low-hapticity arsenic-arene interactions in an intramolecular and multinuclear fashion.

The exact nature of the arsenic-arene interaction warrants examination in the context of the direction of electron flow between the As(III) center and the arene. The π-system of an aromatic ring may act as either an electron donor or acceptor. For example, the cation-π[46] and anion-π[47–50] interactions are well-known examples of arenes acting as Lewis bases or Lewis acids, respectively. Similarly, arsenic(III) may act as either a Lewis base or a Lewis acid. Arsenic(III), particularly in arsines, is easily recognized as a Lewis donor because it is in the same group as nitrogen and phosphorus and similarly often exhibits a stereochemically active lone pair which, in some cases, may participate in coordinative bonding.[40] Proceeding down the Group 15 elements, from nitrogen to bismuth, the Lewis basicity decreases due to increasing localization of the lone-pair electrons in an s-orbital. Likewise, the Lewis acidity of the elements increases on going down the group. The acceptor orbitals responsible for the Lewis acidity may be regarded as three σ^* orbitals oriented 180° opposite the three full bonds of arsenic in a trigonal pyramidal coordination geometry (Figure 1).[51] Arsenic occupies an intermediate position in that neither its Lewis basicity nor its Lewis acidity dominates, and either reactivity pattern may occur.

Two lines of evidence suggest that the arsenic-arene interaction involves electron donation from the π-system of the aromatic ring to the arsenic(III) ion. First, the interaction is primarily observed between arsenic and electron-rich arenes.[52] There is also a corresponding dearth of examples of arsenic interacting with electron-poor arenes. Second, the aromatic ring is often significantly tilted with respect to the three-fold axis of trigonal pyramidal arsenic(III) so that one of the σ^* orbitals is perpendicular to the plane of the aromatic ring.[53] This may be regarded as an orientation that maximizes orbital overlap between the arene-π system and one of the σ^* orbitals.

The directionality of the arsenic-arene interaction with respect to the σ^* orbitals is exemplified in the structure of the $As_2\mathbf{1}_3$ assembly. Looking

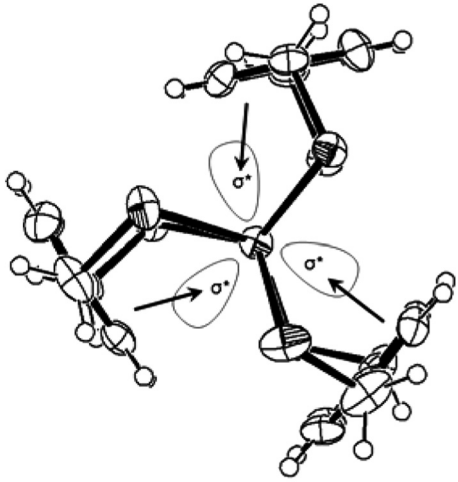

Figure 3. ORTEP representation of the crystal structure of $As_2\mathbf{1}_3$ assembly looking down the As-As axis. Superimposed on this structure are arrows showing the interaction between the aromatic ring of the ligand and the vacant σ^* orbitals on arsenic.

down the As-As axis, each aromatic ring is turned inward so that one side of the aromatic ring is closer to each arsenic ion (Figure 3). The shorter arsenic-arene distances are oriented nearly opposite each As-S bond, in the expected position of the As-S σ^* orbitals.

The crystallization of the $As_2\mathbf{1}_3$ assembly is diastereoselective. There is a chiral axis that runs through each arsenic ion: the three As-S-C bonds around each arsenic ion are bent and tilted like the blades of a propeller. Because each of the arsenic ions has its own chiral axis, the overall chirality of the assembly could in theory be Δ,Δ; Δ,Λ; or Λ,Λ. In the crystalline state, only the *meso*-Δ,Λ diasteromer—which has a plane of symmetry perpendicular to the arsenic-arsenic axis—is observed.

In solution the complex is fluxional. The ^{1}H NMR spectrum of the $As_2\mathbf{1}_3$ assembly shows only one singlet in the aromatic region and one singlet in the methylene region. This is significantly fewer signals than expected for the solid state structure; all of the methylene protons in the static solid state structure are diastereotopic. A dynamic process must be interconverting the diastereomeric protons in solution: the axial chirality at each arsenic ion is rapidly switching. Given the high barrier

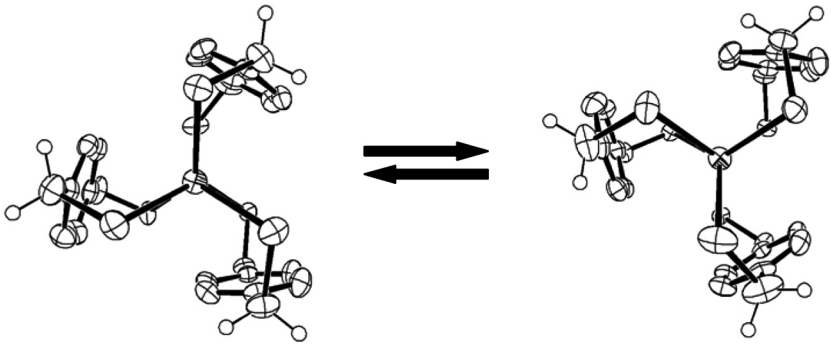

Figure 4. Interconversion between the two conformations of the "meso" $As_2\mathbf{1}_3$ complex likely proceeds via a torsional twist about the As-S-C angle.

to pyramidal inversion of arsines, the most likely mechanism of interconversion involves reversing the twist of each arsenic-sulfur-carbon bond. This interconversion process presumably involves a transition state structure where the C-S-As angle is intermediate between a clockwise and a counterclockwise twist. This process is illustrated in Figure 4.

Although this dynamic process involves reversing the axial chirality at each arsenic center, there is no observed formation of the homoconfigurational Δ,Δ and Λ,Λ diastereomers. The stereochemical inversion at one arsenic ion exhibits mechanical coupling to the stereochemical inversion at the other arsenic ion. The transition state geometry for the interconversion process, therefore, may require all the sulfur and methylene carbons to be in the same plane as the arsenic-arsenic axis. Alternatively, the interconversion may proceed in two steps with each individual metal center inverting separately, albeit with the concentration of the transient intermediate too low to measure.[54]

Syn- and *Anti*-$As_2\mathbf{1}_2Cl_2$ Macrocycles

In the absence of base, 1,4-bis(mercaptomethyl)benzene ($H_2\mathbf{1}$) and $AsCl_3$ assemble into a mixture of *syn*- and *anti*-$As_2\mathbf{1}_2Cl_2$ macrocycles (Figures 5 and 7). The macrocycles exist as an equilibrium mixture of *syn*- and *anti*-diastereomers in solution, although the individual isomers can be crystallized selectively. Pentane diffusion into a $CHCl_3$ solution of $AsCl_3$ and $H_2\mathbf{1}$ under different conditions of concentration and stoichiometry allowed selective crystallization of the individual isomers.[18]

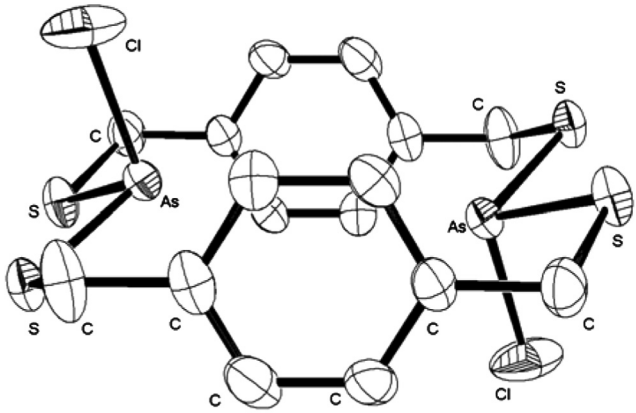

Figure 5. ORTEP representation of the crystal structure of the *anti*-$As_2\mathbf{1}_2Cl_2$ macrocycle. Cocrystallized $AsCl_3$ is omitted from the diagram.

In the presence of excess $AsCl_3$, the *anti*-macrocycle selectively crystallizes as an $AsCl_3$ solvate. A mixture of $H_2\mathbf{1}$ and $AsCl_3$ at higher concentrations produces crystals containing exclusively the *syn*-diastereomer.

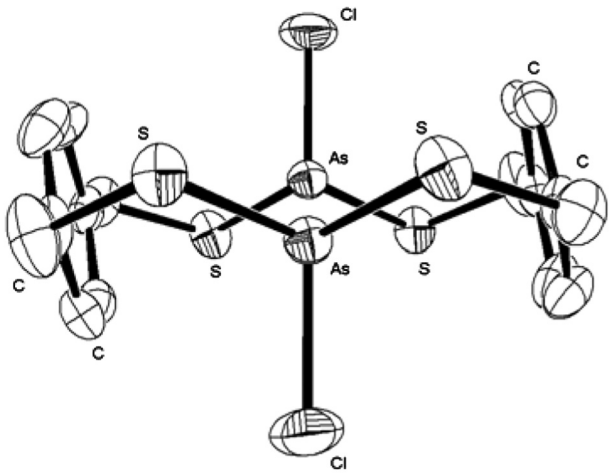

Figure 6. ORTEP representation of the cystal structure of the *anti*-$As_2\mathbf{1}_2Cl_2$ macrocycle looking down the As-As axis. Cocrystallized $AsCl_3$ is omitted from the diagram.

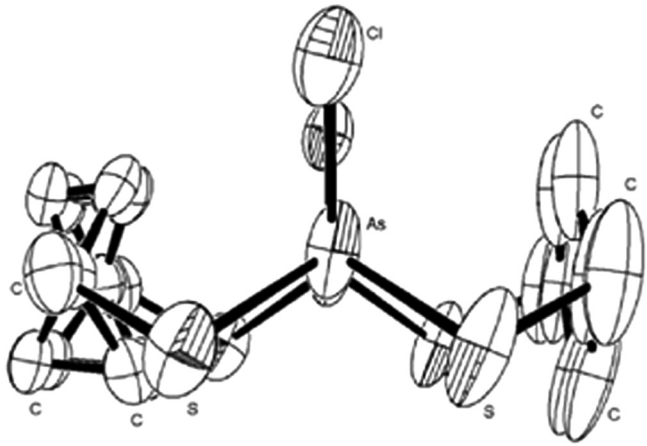

Figure 7. ORTEP representation of the crystal structure of the *syn*-$As_2\mathbf{1}_2Cl_2$ macrocycle looking down the As-As axis. Rotational disorder of the left phenyl ring has been modeled as partial occupancy in two different orientations.

The crystal structures of the *anti*- and *syn*-macrocycles are shown in Figures 5 and 7, respectively. The arsenic-π attraction is again evident in these dinuclear As(III) structures. Arsenic-arene distances are as short as 3.165 Å, which is less than the sum of the van der Waals radii of arsenic and carbon. Therefore, each arsenic ion is participating in arsenic-arene secondary bonding interactions with two aromatic rings.

Given the approximations inherent in van der Waals and ionic radii, definite assignment of a secondary interaction is strengthened by additional lines of evidence.[55] Possibly, the strongest additional evidence for a given secondary interaction is spectroscopic observation of association in solution. The well-known infrared spectroscopic signature of hydrogen bonding is an archetypal example. In the case of the arsenic-π interaction, there is some solution NMR evidence[56] and some limited solid-state infrared spectroscopy supporting the existence of the arsenic-π interaction. In many cases, however, it is necessary and convenient to assign secondary bonding interactions solely on atomic coordinates derived from the material in the solid state—both to understand the forces influencing crystal packing and in cases where competitive solvation makes measurement in solution difficult.

In addition to short contact distances between atoms, secondary bonding interactions are corroborated in the solid state by considering

the orientations of reactive orbitals on the interacting species (Figure 1). The strongest arguments for secondary interactions in the solid state involve species in orientations such that their orbitals are clearly aligned to allow for an interaction. The case is considerably bolstered when it can be shown that the participating atoms are distorted out of place in order to maximize the interaction. The orientation of reactive orbitals should be appropriate and, depending on the proposed strength of the interaction, there should be structural distortion consistent with that interaction.

The crystal structure of *syn*-$As_2\mathbf{1}_2Cl_2$ is shown in Figures 5 and 6. The arsenic-arsenic distance is 5.02 Å and each arsenic ion makes close contact with two carbons of each aromatic ring of the ligand. Considering the nature of the arene-arsenic donor-acceptor interaction (see above), one might expect each aromatic ring to be tilted slightly inward to make better contact with the presumed acceptor σ^* orbitals on each arsenic ion. Unfortunately, considerable disorder of the positions of the arene carbons makes it difficult to draw conclusions regarding whether the interaction is influencing the lay of the aromatic rings (Figure 6). Regardless, the nearly parallel orientation of the two arene rings and their proximity to the As(III) ions suggest that the necessary orbitals are in an appropriate geometry for an η^2-secondary interaction.

The crystal structure of the *anti*-macrocycle is shown in Figure 7. The arsenic-arsenic distance in this diastereomer is shorter—4.65 Å. Each arsenic ion makes close contact with two carbon atoms of each aromatic ring of the ligand. The two aromatic rings of the macrocycle are again nearly parallel. Presumably, any movement of one aromatic ring to make better contact with one σ^* orbital would weaken contact with another σ^* orbital on the other arsenic ion. Still, the closest As(III)-C_{ortho} distances do occur opposite an As-S bond, in the expected vicinity of an acceptor As-S σ^* orbital. Despite the lack of dramatic structural distortions, the necessary orbitals are again in an orientation appropriate for η^2-secondary interactions.

The presence of multiple arsenic-arene interactions enforces unexpectedly short arsenic-arsenic distances in each macrocycle. CAChe molecular mechanics minimizations (MM2, MM3)—which do not take arsenic-arene secondary interactions into account—suggest that the arsenic-arsenic distance would be no less than ca. 6 Å. The crystal structure shows the influence of the arsenic-arene interactions: the arsenic atoms are significantly drawn into the center of the macrocyclic cavity

with an arsenic-arsenic distance of only 5.02 Å in the *syn*-macrocycle and only 4.65 Å in the *anti*-isomer.

Controlling Diastereomeric Excess in $As_2L_2Cl_2$ Macrocycles

Similar to the 1,4-bis(mercaptomethyl)benzene system described above, three isomeric naphthalene-based ligands, 2,6-bis(mercaptomethyl)-naphthalene (H_2**2**), 1,5-bis(mercaptomethyl)naphthalene (H_2**3**), and 1,4-bis(mercaptomethyl)naphthalene (H_2**4**) (Figure 8), were each reacted with $AsCl_3$ to form self-assembled equilibrium mixtures of *syn*- and *anti*-macrocycles. By using these ligands, which differ only by the ring positions of the mercaptomethyl groups, we were able to access different ratios of the two macrocyclic isomers including mostly *syn*, mostly *anti*, and an almost statistical mixture of the two.[57]

Within these macrocycles, the arsenic-π interaction causes the arsenic atom and its coordination sphere, to be pulled toward the ligand backbone. Some steric congestion is present around the chlorine and sulfur atoms (Figure 9), and the diastereomer with the least amount of unfavorable steric strain forms in excess (giving rise to a diastereomeric excess, de). The de of these macrocycles in solution has been measured using ^{1}H NMR spectroscopy and found to be only 9% for As_2**2**$_2Cl_2$ (it is not known which isomer is in excess). Neither the crystal structure nor the computer models indicate any steric strain in either isomer, so the small de is not surprising. Crystals were obtained of *anti*-As_2**2**$_2Cl_2$ (Figure 10a) and the structure reveals a clear arsenic-π interaction within a cavity that is too small to accommodate any guests screened to date (metal cations, H^+ or small organic molecules).

Anti-As_2**3**$_2Cl_2$ exists in 85% de in solution as determined by ^{1}H NMR spectroscopy. The observed excess seen for this macrocycle

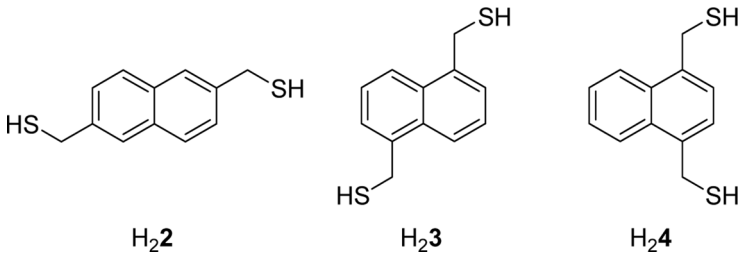

H_2**2** H_2**3** H_2**4**

Figure 8. Isomeric naphthalene-based dithiol ligands.

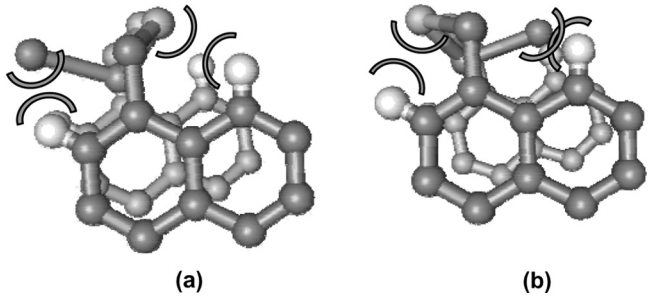

Figure 9. Partial ball and stick models showing the steric repulsions between chlorine and sulfur atoms when the chlorine atom is pointing (a) away from and (b) toward the hydrocarbon backbone of the ligand.

can be attributed to the large difference in steric interactions between the chlorine atom and the naphthalene backbone of the ligand when the Cl is pointing into the cavity (toward C-H) or pointing out (toward H). Again, crystals were obtained and found to be 100% *anti* (Figure 10b).

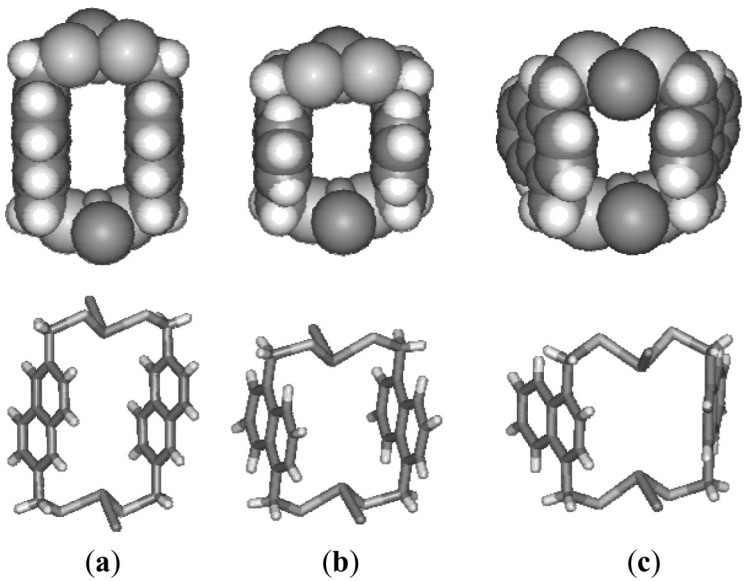

Figure 10. Representations of single-crystal X-ray structures of $As_2L_2Cl_2$ macrocycles derived from naphthalene-based ligands. Space filling and wireframe representations of (a) *anti*-$As_2\mathbf{2}_2Cl_2$, (b) *anti*-$As_2\mathbf{3}_2Cl_2$ and (c) *syn*-$As_2\mathbf{4}_2Cl_2$ macrocycles.

In the case of $As_2\mathbf{4}_2Cl_2$ macrocycles a 90% de of the *syn* macrocycles exists in solution. In the solid state, however, the *syn* isomer crystallizes exclusively (Figure 10c). Diastereocontrol is important in our design scheme to utilize macrocycles as synthons for larger assemblies. For instance, *syn*-macrocycles are preorganized to form larger discrete assemblies allowing us to study host-guest chemistry, while *anti*-macrocycles can be functionalized to provide extended structures. We are currently pursuing this goal, as well as trying to design ligands that will form arsenic-containing macrocycles with improved diastereocontrol.

Supramolecular $Sb_2L_2Cl_2$ Assemblies

Antimony is also able to participate in self-assembly with dithiol ligands. In the absence of base, 1,4-bis(mercaptomethyl)benzene ($H_2\mathbf{1}$) and antimony(III) form a dinuclear $Sb_2\mathbf{1}_2Cl_2$ complex (Figure 11). This macrocycle also exhibits pnictogen-arene interactions: each antimony(III) ion participates in an η^2-secondary interaction with one aromatic ring of the macrocycle and an η^3-secondary interaction with the opposite ring.[58] The shortest Sb-C interactions are again opposite an antimony-sulfur bond consistent with the view that the π-cloud of the arene ring is donating into the Sb-S σ^* orbital (Figure 11). For example, the Sb-C_{ortho}

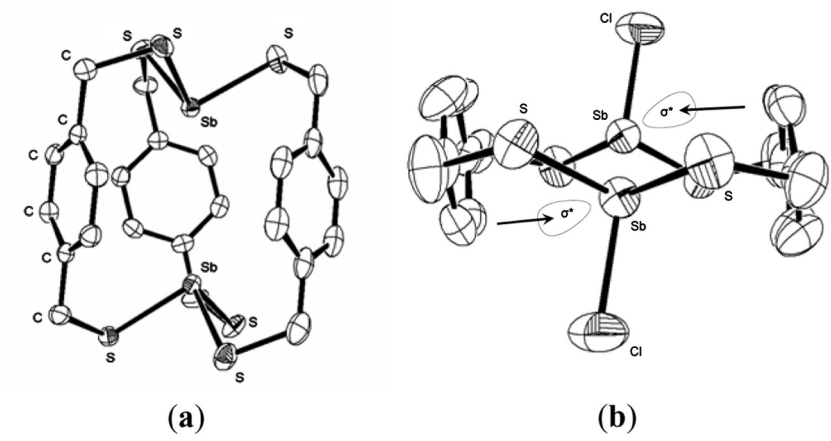

Figure 11. ORTEP representation of the single crystal X-ray structure of (a) $Sb_2\mathbf{1}_3$ and (b) $Sb_2\mathbf{1}_2Cl_2$.

distance opposite the Sb-S bond is 3.50 Å versus 3.61 Å for the other *ortho*-carbon atom. Since the antimony-chlorine bonds point away from, and bisect the two As-S bonds, regardless of the way the two arene rings are canted, there will always be two *ortho*-carbon atoms positioned closer to the antimony ions than the other two.

Similarly to the case for arsenic, the deprotonated thiolate ligands assemble with $SbCl_3$ to form an $Sb_2\mathbf{1}_3$ complex. Interestingly, this assembly is chiral and posesses a helical twist, crystallizing as a racemic mixture of enantiomers (Figure 11). The Sb-Sb distance in this complex is only 4.30 Å, due to stronger antimony-π interactions. To achieve this proximity between antimony atoms, the ligand must adopt a helical twist to "compress" the complex. As in the case for $As_2\mathbf{1}_3$, a dynamic torsional rotation interconverts the two enantiomers in solution. Although the *meso* conformer of this complex has not been observed, it could also be in fast equilibrium with the helical conformers in solution on the NMR timescale.

The crystal structure of $Sb_2\mathbf{1}_3$ readily demonstrates the presence of many intramolecular Sb-arene secondary interactions. Each Sb(III) ion makes close contacts with two carbons of each of the three aromatic rings. The orientations of these close contacts are consistent with the expected positions of available reactive orbitals. Furthermore, the assembly bears further structural evidence consistent with electronic donation from the π-system into the Sb-S σ^* orbital. Each aromatic ring is twisted inward in manner that maximizes contact between the ring carbons and the expected positions of the Sb-S σ^* orbitals (Figure 11).

III. MONONUCLEAR ARSENIC COMPLEXES: PROBING SBI'S IN ARSINE COMPLEXES

Secondary Bonding Interactions Between Arsenic and the Imido Oxygen of β-Mercaptoethylimidonaphthalene

Single crystals suitable for X-ray analysis were obtained for H**5**, $As\mathbf{5}_2Cl$ and $As\mathbf{5}_3$ by either slow evaporation of chloroform to obtain H**5** or rapid addition and mixing of $AsCl_3$ into a solution of **5** (Figure 12).[59] Interestingly, the crystal structures of $As\mathbf{5}_2Cl$ and $As\mathbf{5}_3$ did not reveal secondary bonding interactions between arsenic and the aromatic rings as expected. Instead, one of the imido oxygens was located in close proximity to the arsenic metal center causing a slightly higher energy gauche

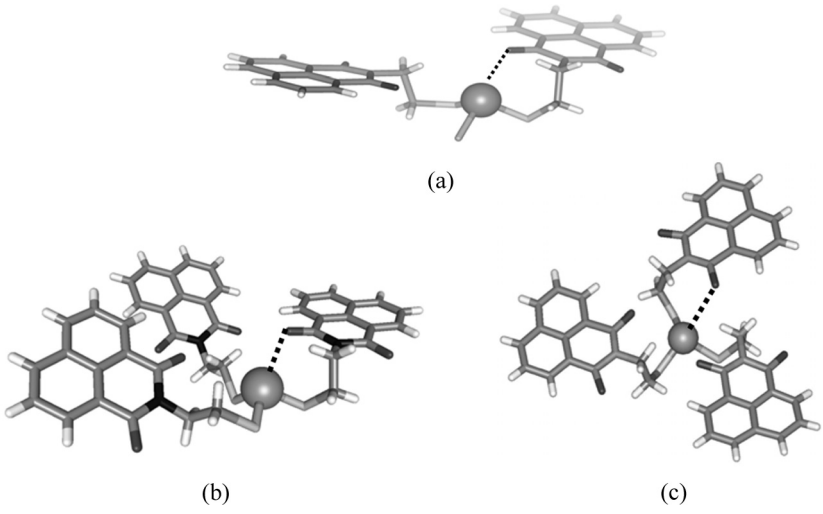

Figure 12. Wireframe representations of crystal structures of three arsenic complexes formed from **5**. Secondary bonding interactions are denoted by dashed linse. (a) As**5**$_2$Cl with As···O distance of 2.91 Å. (b) As**5**$_3$ with As···O distance of 3.21 Å. and (c) C_3 symmetric polymorph of As**5**$_3$ with As···O distance of 3.16 Å.

conformation in the ethyl group of the ligands (Figure 12a and 12b). The observed As···O distances (2.91 Å and 3.21 Å for As**5**$_2$Cl and As**5**$_3$, respectively) are less than the sum of the van der Waals radii of As-S, and thus within the accepted range for SBI's.[60,61] Furthermore, the oxygen atoms are directly opposite the As-S or As-Cl bonds, indicating interaction with a σ^* orbital.

The As-Cl bond length of 2.25 Å for the As-Cl opposite the weakly bound oxygen in As**5**$_2$Cl (Figure 12a) falls within the expected value.[61] However, a search of the Cambridge Structure Database (CSD)[62,63] for structures containing $AsCl_x$ with observed SBI's produced a wide range of bond elongations. The measured value of 2.25 Å falls between 2.19 Å for As-Cl bonds that do not experience weak SBI's and 2.38 Å for an As-Cl bond opposite a weakly bound heteroatom. A slight As-S elongation was observed in the C_3 symmetric complex As**5**$_3$: 2.25 Å verses 2.22 Å for the non-SBI As-S bond in the unsymmetrical As**5**$_3$ complex (Figure 12c). (An insignificant bond elongation of 0.01 Å was observed in the unsymmetrical As**5**$_3$ complex.) In some reported crystal structures, As-Cl bond lengths of 2.54 Å have been observed. Therefore, the extent of bond

lengthening can be qualitatively related to the strength of the secondary bonding interaction of the heteroatom responsible for the observed perturbation.

In addition to the examples mentioned above from the literature describing SBI's, a search of the (CSD) revealed organoarsenic structures containing As···O distances similar to the observed ranges of the β-mercaptoimido-arsenic complexes. It is interesting that in order to accommodate such an interaction, at least one ligand for each complex resides in the higher energy *gauche* conformation in the solid state. Although this barrier may only require 1 kcal/mol or less to overcome, the As···O interaction is strong enough to maintain its conformation during crystallization thus resulting in a nonparallel arrangement between the planes of aromatic stacking formed by the naphthalene core. This arrangement differs from the crystal packing of the β-mercaptoimido ligand alone.

A different polymorph of As**5**$_3$ was obtained by slow diffusion of $AsCl_3$ into a solution containing deprotonated ligand 5 (Figure 12c). The resulting complex was found to be C_3-symmetric with the imido oxygens from all three ligands participating in SBI's and an As···O distance of 3.16 Å. This is less than that of As**5**$_2$Cl and the non-C_3-symmetric As**5**$_3$ complex of 3.21 Å (Figure 12b). As mentioned above, the alkyl linkage of each ligand in this polymorph is forced into the higher energy gauche conformation, accounting for a 2–3 kcal/mol increase in energy as well as nonparallel π-stacking crystal planes.

Spectroscopic Studies of Organoarsenic Complex

In addition to demonstrating SBI's between arsenic and the naphthalimide core—which was chosen for its well known electronic absorption and emission properties—interesting spectroscopic properties were recorded. Previous work by our group[17] and by Schmidbaur and coworkers[52] demonstrated the ability of arsenic to exhibit through-space interactions with aromatic π-systems. It was hypothesized that the naphthalene core would interact with arsenic by an arsenic-π secondary bonding interaction due to the close proximity of the ligand to the metal center. It was therefore believed that the interaction should impart a change in the spectral properties of the naphthalimide core, resulting in a shift in the ultraviolet (UV) absorption spectrum. The basis of such an observation can be explained by a charge transfer between the

π-orbitals of the aromatic ring system to the σ^* orbitals of arsenic.[64] The expected spectral shifts are dependant on the direction of flow of electron density. A bathochromic (or lower energy) shift will result from a metal to ligand interaction caused by a decrease in the energy gap between ground and excited states of the ligand as a result of increased electron density in the aromatic chromophor.[65] A hypsochromic (or higher energy) shift will be observed due to a ligand to metal interaction as seen between arsenic and a dithiocarboxylate ligand studied by Tani and coworkers.

Upon addition of arsenic trichloride to a 2:1 dichloromethane/methanol solution containing deprotonated β-mercaptoimido ligand, no such shift in wavelength was observed in the two prominent peaks at λ_{238} and λ_{335} nm (Figure 13). However, an increase in peak height at λ_{335} was observed to give a peak ratio of 0.81 (relative height of P_{335}/P_{238}) after deprotonation with solid KOH. This is considerably larger than a peak ratio of 0.67 for the protonated β-mercaptoimido ligand. The addition of base causes the nearly colorless solution of **H5** to appear bright yellow. Upon addition of $AsCl_3$, the yellow solution becomes colorless once again as the $As\mathbf{5}_3$ complex forms. The UV-Vis spectrum of $As\mathbf{5}_3$ has a peak ratio of 0.49, slightly smaller than the native ligand

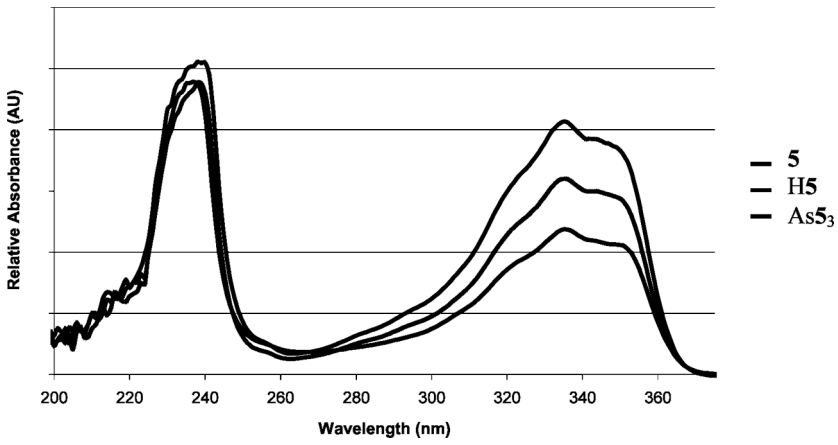

Figure 13. UV spectra of deprotonated ligand **5**, protonated ligand **H5**, and $As\mathbf{5}_3$ in a 2:1 dichloromethane:methanol solution. Relative peak height ratios were determined by P_{335}/P_{238} to give 0.81, 0.67 and 0.49, respectively.

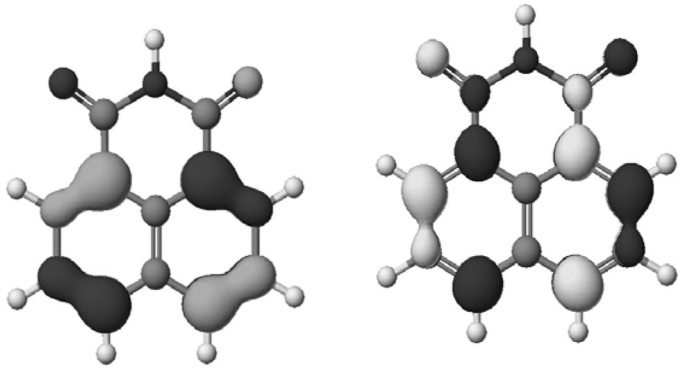

Figure 14. CAChe computational calculations of the HOMO (a) and LUMO (b) of 1,8-naphthalimide. A node is present at the imide nitrogen for both models. This limits the orbital mixing between the conjugated imide and nitrogen substituents.

(Figure 13). Using the peak at λ_{238} as an indicator to qualitatively assume similar concentrations between solutions, a change in absorption must be due in part to a change in the molar extinction coefficient (ε) at λ_{238}. This is in good agreement with respect to similar perylene-based[66] systems where the observed trend is attributed to nodes in the HOMO and LUMO at the imide nitrogen resulting in a reduction in orbital mixing between the imide and the substituents of the imide (Figure 14); therefore no peak shift is observed.

The likely change in extinction coefficient has been attributed to changes in vibronic motions, dubbed the "loose bolt effect."[67] Essentially, bulkier groups off the imide nitrogen cause a decrease in vibronic motion and thus a decrease in the extinction coefficient. Upon complex formation, the addition of the heavier arsenic results in a decreased extinction coefficient as observed; therefore, changes in peak height are most likely not the result of an inductive effect on the imide nitrogen as a result of the changing environment of the thiol moiety. The change in molar extinction coefficient can also be explained by the observed color change between solutions; as ε increases, the underlying yellow color of the deprotonated ligand becomes more apparent.

Regardless of the nature of the observed changes in peak heights, peak migration did not occur. This suggests that arsenic is not perturbing the spectral properties of the naphthalimide ligand as expected. The lack

of electronic interaction might be explained by the ability of the ligands to freely rotate in space, which is not conducive in promoting As-π interactions. Locking the conformation of the surrounding ligands to arsenic should enhance the likelihood of an electronic interaction and result in corresponding spectral changes.[68] Ligands that undergo spectral changes might find utility in sensor applications; a sensor that loses color due to complex formation is equivalent in usefulness to a sensor that undergoes a color change. Can a supramolecular sensor be designed that either "turns on" (or turns off) upon self-assembly with arsenic or other main group elements? One example of commercially available biarsenical fluorophores utilizes PET quenching with arsenic and tetracysteines for near off/on fluorescene.[68]

CONCLUSION

Our work continues to focus on the design and synthesis of organothiol ligands for use in supramolecular coordination chemistry of arsenic and other main group elements. The lack of efficient chelators for toxic ions such as arsenic drive this work forward and the use of supramolecular chemistry provides for a different approach to arsenic sequestering. Metal binding specificity and interesting emergent spectral properties comprise two encouraging results we have observed thus far in this line of research. We are optimistic that rich host-guest chemistry and new structures types are soon to follow on the basic science end of this research. Applications in sensing stemming from a supramolecular approach to metal chelation will be investigated, and we are currently exploring the use of these ligands to provide nanostructured materials for use as sorbents for water purification.[69]

ACKNOWLEDGMENT

We gratefully acknowledge the National Science Foundation for a CAREER award (CHE-0545206), the Medical Research Foundation of the Oregon Health and Sciences University and the University of Oregon for generous financial support of the research reviewed herein. D.W.J is a Cottrell Scholar of Research Corporation. T.G.C. and W.J.V. acknowledge the NSF for Integrative Graduate Education and Research Traineeships.

REFERENCES

1. Lehn, J.-M., 2002. Introductory perspective toward complex matter: Supramolecular chemistry and self-organization. *Proc. Natl. Acad. Sci. U. S. A.*, **99**, 4763–4768.
2. Vignon, S. A., T. Jarrosson, T. Iijima, H.-R. Tseng, J. K. M. Sanders, and J. F. Stoddart, 2004. Switchable neutral bistable rotaxanes. *J. Am. Chem. Soc.*, **126**, 9884–9885.
3. Caulder, D. L. and K. N. Raymond, 1999. The rational design of high symmetry coordination clusters. *J. Chem. Soc., Dalton Trans*, 1185–1200.
4. Fiedler, D., D. H. Leung, R. G. Bergman, and K. N. Raymond, 2005. Selective molecular recognition, C-H bond activation, and catalysis in nanoscale reaction vessels. *Acc. Chem. Res.*, **38**, 349–358.
5. Hamilton, T. K. and L. R. MacGillivray, 2004. Enclosed chiral environments from self-assembled metal-organic polyhedra. *Cryst. Growth Des.*, **4**, 419–430.
6. Turner, D. R., A. Pastor, M. Alajarin, and J. W. Steed, 2004. Molecular containers: design approaches and applications. *Struct. Bonding*, **108**, 97–168.
7. Hof, F., S. L. Craig, C. Nuckolls, and J. Rebek, Jr. 2002. Molecular encapsulation. *Angew. Chem. Int. Ed.*, **41**, 1488–1508.
8. Spessard, G. O. and G. L. Miessler, 2000. *Organometallic Chemistry*, Prentice-Hall Inc., Upper Saddle River, NJ.
9. Piguet, C., C. Edder, S. Rigault, G. Bernardinelli, J. G. Bunzli, and G. Hopfgartner, 2000. Isolated d-f pairs in supramolecular complexes with tunable structural and electronic properties. *J. Chem. Soc., Dalton Trans.*, 3999–4006.
10. Holliday, B. J. and C. A. Mirkin, 2001. Strategies for the construction of supramolecular compounds through coordination chemistry. *Angew. Chem.*, **40**, 2022–2043.
11. Orr, G. W., L. J. Barbour, and J. L. Atwood, 1999. Controlling molecular self-organization: Formation of nanometer-scale spheres and tubules. *Science*, **285**, 1049–1052.
12. Sun, X., D. W. Johnson, K. N. Raymond, and E. H. Wong, 2001. A silver-linked supramolecular cluster encapsulating a cesium cation. *Inorg. Chem.*, **40**, 4504–4506.
13. Radhakrishnan, U. and P. J. Stang, 2003. Synthesis and characterization of cationic iodonium macrocycles. *J. Org. Chem.*, **68**, 9209–9213.
14. Paver, M. A., J. S. Joy, and M. B. Hursthouse, 2002. A twenty-four membered mixed-metal macrocycle; synthesis and structure of *cyclo*-[(3-Me-1,2-$C_6H_3O_2)_2SbNa(THF)_2]_6$. *Chem. Commun.*, 2150–2151.
15. Garcia, A. M., F. J. Romero-Salguero, D. M. Bassani, J.-M. Lehn, G. Baum, and D. Fenske, 1999. Self-assembly and characterization of multimetallic grid-type lead(II) complexes. *Chem. Eur. J.*, **5**, 1803–1808.

16. Marcovich, D., E. N. Duesler, R. E. Tapscott, and T. F. Them, 1982. Stereochemistry of arsenic(III) and antimony(III) 1,2-dihdroxycyclohexane-1,2-dicarboxylates. *Inorg. Chem.*, **21**, 3336–3341.
17. Vickaryous, W. J., R. Herges, and D. W. Johnson, 2004. Arsenic- π interactions stabilize a self-assembled As_2L_3 supramolecular complex. *Angew. Chem., Int. Ed.*, **43**, 5831–5833.
18. Vickaryous, W. J., E. R. Healey, O. B. Berryman, and D. W. Johnson, 2005. Synthesis and characterization of two isomeric, self-assembled arsenic-thiolate macrocycles. *Inorg. Chem.*, **44**, 9247–9252.
19. Kerr, P. G., P. H. Leung, and S. B. Wild, 1987. Optically-active arsenic macrocycles – stereospecific syntheses of enantiomers and diastereomers of 14-membered trans-As_2S_2 chelating macrocycles containing resolved asymmetric tertiary arsine donors. *J. Am. Chem. Soc.*, **109**, 4321–4328.
20. Shaikh, T. A., R. C. Bakus, S. Parkin, and D. A. Atwood, 2006. Structural characteristics of 2-halo-1,3,2-dithiarsenic compounds and tris-(pentafluorophenylthio)-arsen. *J. Organomet. Chem.*, **691**, 1825–1833.
21. Shaikh, T. A., S. Parkin, and D. A. Atwood, 2006. Synthesis and characterization of a rare arsenic trithiolate with an organic disulfide linkage and 2-chloro-benzo-1,3,2-dithiastibole. *J. Organomet. Chem.*, **691**, 4167–4171.
22. Alcock, N. W. 1972. *Secondary Bonding to Nonmetallic Elements*. Academic Press, Inc., New York.
23. Pitt, M. A. and D. W. Johnson, 2007. Main group supramolecular chemistry. *Chem. Soc. Rev.*, DOI:10.1039/b610405n, **46**, 1441–1453.
24. Aposhian, H. V. and M. M. Aposhian, 2005. Arsenic toxicology: Five questions. *Chem. Res. Toxicol.*, **18**, 1287–1295.
25. Magalhães, M. C. F. 2002. Arsenic. An environmental problem limited by solubility. *Pure Appl. Chem.*, **74**, 1843–11850.
26. Hindmarsh, J. T., C. O. Abernathy, G. R. Peters, and R. F. McCurdy, 2002. Environmental aspects of arsenic toxicity, In *Heavy Metals in the Environment*, Sarkar, B. (ed.), pp 217–229, Marcel Dekker, Inc., New York.
27. Bhattacharya, P., G. Jacks, S. H. Frisbie, E. Smith, R. Naidu, and B. Sarkar, 2002. *Arsenic in the Environment: A Global Perspective*. Marcel Dekker, Inc., New York.
28. Roy, P. and A. Saha, 2002. Metabolism and toxicity of arsenic: A human carcinogen. *Curr. Sci.*, **82**, 38–45.
29. Hossain, M. F. 2006. Arsenic contamination in Bangladesh—an overview. *Agricult. Ecosys. Environ.*, **113**, 1–16.
30. Mandal, B. K. and K. T. Suzuki, 2002. Arsenic round the world: A review. *Talanta*, **58**, 201–235.
31. Frisbie, S. H., R. Ortega, D. M. Manynard, and B. Sarkar, 2002. The concentrations of arsenic and other toxic elements in Bangladesh's drinking water. *Environ. Health Perspect.*, **110**, 1147–1153.

32. Hinkle, S. R. and D. J. Polette, 1999. *Arsenic in Ground Water of the Willamette Basin, Oregon* 98-4205, USGS, Portland.
33. Solis, A. R., R. Mukopadhyay, B. P. Rosen, and T. L. Stemmler, 2004. Experimental and theoretical characterization of arsenite in water: Insights into the coordination environment of As-O. *Inorg. Chem.*, **43**, 2954–2959.
34. Cullen, W. R. and K. J. Reimer, 1989. Arsenic speciation in the environment. *Chem. Rev.* **89**, 713–764.
35. Silver, S. and L. T. Phung, 2005. Genes and enzymes involvced in bacterial oxidation and reduction of inorganic arsenic. *Appl. Environ. Microbiol.*, **71**, 599–608.
36. Adams, S. R., R. E. Campbell, L. A. Gross, B. R. Martin, G. K. Walkup, Y. Yao, J. Llopis, and R. Y. Tsien, 2002. New biarsenical ligands and tetracysteine motifs for protein labeling in vitro and in vivo: Synthesis and biological applications. *J. Am. Chem. Soc.*, **124**, 6063–6076.
37. Cruse, B. W. T. and M. N. G. James, 1972. The crystal structure of the arsenite complex of dithiothreitol. *Acta Cryst.*, **B28**, 1325–1331.
38. Farrer, B. T., C. P. McClure, J. E. Penner-Hahn, and V. L. Pecoraro, 2000. Arsenic(III)-cysteine interactions stabilize three-helix bundles in aqueous solution. *Inorg. Chem.*, **39**, 5422–5423.
39. Garje, S. S. and V. K. Jain, 2003. Chemistry of arsenic, antimony and bismuth compounds derived from xanthate, dithiocarbamate and phosphorous based ligands. *Coord. Chem. Rev.*, **236**, 35–56.
40. Trialkyl arsine complexes are well known to coordinate metal ions through the lone pair on arsenic. Therefore, this lone pair cannot entirely be considered as inert. As a representative example, triphenylarsines participate in dative bonding to platinum(II) in the complexes $PtI_3(AsPh_3)$ and $PtI_2(AsPh_3)$pyr, see: Kuznik, N., Wendt, O. F. 2002. The *trans* effect and *trans* influence of triphenyl arsine in platinum(II) complexes. A comparative mechanistic and structural study. *J. Chem. Soc. Dalton Trans.*, **15**, 3074–3078.
41. Alcock, N. W. 1990. *Bonding and Structure: Structural Principles in Inorganic and Organic Chemistry.* Ellis Horwood, New York.
42. SBI's occur within the sum of the van der Waals radii (Bondi, A. 1964. Van der waals volumes and radii. *J. Phys. Chem.*, **68**, 441–451) of two or more atoms, and can offer a potentially powerful method toward ligand design to optimize chelation of main-group metals: Srivastava, P. C. 2005. Secondary bonding, C-H- - -O hydrogen bonding assisted supramolecular associations and charge transfer (CT) complexes of organotelluriums and their nonlinear optical properties. *Phosphorus, Sulfur Silicon Relat. Elem.*, **180**, 969–983.
43. Hof, F. and J. Rebek, Jr. 2002. Molecules within molecules: Recognition through self-assembly. *Proc. Natl. Acad. Sci. U. S. A.*, **99**, 4775–4777.
44. Tani, K., S. Hanabusa, S. Kato, S. Mutoh, S. Suzuki, and M. Ishida, 2001. Thioacylsulfanylarsines $(RCS_2)_xAsPh_{3-x}$, $x = 1$–3: Synthesis, structures,

natural bond order analyses and reactions with piperidine. *J. Chem. Soc. Dalton Trans.*, 518–527.

45. Probst, T., O. Steigelmann, J. Riede, and H. Schmidbaur, 1991. Arsenic(III), antimony(III), and bismuth(III) trihalide complexes of [2.2.2]paracyclophane: From weak centroid van der Waals coordination to strongly directional π complexation with single or double external η^6-coordination. *Chem. Ber.*, **124**, 1089–93.
46. Ma, J. C. and D. A. Dougherty, 1997. The cation-π interaction. *Chem. Rev.*, **97**, 1303–1324.
47. Alkorta, I., I. Rozas, and J. Elguero, 2002. Interaction of anions with perfluoro aromatic compounds. *J. Am. Chem. Soc.*, **124**, 8593–8598.
48. Mascal, M., A. Armstrong, and M. D. Bartberger, 2002. Anion-aromatic bonding: A case for anion recognition by π-acidic rings. *J. Am. Chem. Soc.*, **124**, 6274–6276.
49. Quiñonero, D., C. Garau, C. Rotger, A. Frontera, P. Ballester, A. Costa, and P. M. Deyá, 2002. Anion-π interactions: Do they exist? *Angew. Chem. Int. Ed.*, **41**, 3389–3392.
50. Berryman, O. B., V. S. Bryantsev, D. P. Stay, D. W. Johnson, and B. P. Hay, 2007. Structural criteria for the design of anion receptors: The interaction of halides with electron-deficient arenas. *J. Am. Chem. Soc.*, **129**, 48–58.
51. Alkyl substituted arenes are the most common examples: Carmalt, C. J., N. C. Norman, 1998. Arsenic, antimony, and bismuth: Some general properties and aspects of periodicity. In *Chemistry of arsenic, Antimony, and Bismuth*, Norman, N. C. (ed.), pp. 1–38, Blackie Academic & Professional, London.
52. Schmibaur, H., R. Nowak, O. Steigelmann, and G. Muller, 1990. Pi-complexes of p-block elements: Synthesis and structures of adducts of arsenic and antimony halides with alkylated benzenes. *Chem. Ber.*, **123**, 1221–1226.
53. Alkyl substituted arenes are the most common examples: Camerman, A., and J. Trotter, 1965. Stereochemistry of arsenic. 13. 10-chloro-5,10-dihydrophenarsazine, *J. Chem. Soc.*, 730–738.
54. This behavior has been discussed in regard to gallium catecholamides: Kersting, B., M. Meyer, R. E. Powers, and K. N. Raymond, 1996. Dinuclear catecholate helicates: Their inversion mechanism. *J. Am. Chem. Soc.*, **118**, 7221–7222.
55. A short interatom distance, less than the sum of the van der Waals radii, does not necessarily mean the two atoms are participating in a secondary bonding interaction. The values given in tables of van der Waals radii involve several assumptions and are averaged for elements in many different compounds. The authors of commonly cited tables of van der Waals radii themselves caution in the very papers so cited that their values are averages involving many approximations (see: Bondi, A. 1964. Van der waals olumes and radii.

J. Phys. Chem. **68**, 441–451; Shannon, R. D. 1976. Revised effective ionic radii and systematic studies of interatomic distances in halides and chalcogenides. *Acta Cryst.*, **A32**, 751–67). For example, tables of van der Waals radii begin with the assumption that the atoms are spherical. Furthermore, the radius of a given atom is assumed to be invariant regardless of factors including: different substituents, different numbers of bonds, different oxidations states, different phases, and different orientations. An atom is assigned the same radius regardless of these factors, even though this is inaccurate. An example famously given to illustrate the variation of van der Waals radius with orientation involves carbon tetrachloride (see: Pauling, L. C. 1960. *The Nature of the Chemical Bond and the Structure of Molecules and Crystals. An Introduction to Modern Structural Chemistry, 3rd ed.*). The chlorine atoms in carbon tetrachloride are 2.87 Å apart, significantly shorter than the sum of their van der Waals radii (3.6 Å), yet Pauling observes that CCl_4 does not show any of the properties that would be associated with the great strain resulting from the repulsion between such close chlorine atoms. The van der Waals radius in directions close to the bond (C-Cl bond in this case) is less.

56. Vakhrin, M. I. and V. S. Grechishkin, 1974. Complexing of substituted benzenes with arsenic trichloride studied by a nuclear magnetic resonance method. *Zh. Fiz. Khim.*, **48**, 1515–17.
57. Cangelosi, V. M., A. C. Sather, L. N. Zakharov, O. B. Berryman, and D. W. Johnson, 2007. Diastereoselectivety in the self-assembly of $As_2L_2Cl_2$ macrocycles is directed by the As-π interaction. *Inorg. Chem*, in press.
58. Vickaryous, W. J., L. N. Zakharov, and D. W. Johnson, 2006. Self-assembled antimony-thiolate Sb_2L_3 and $Sb_2L_2Cl_2$ complexes. *Main Group Chem.*, **5**, 51–59.
59. Carter, T. G., E. R. Healey, M. A. Pitt, and D. W. Johnson, 2005. Secondary bonding interactions observed in two arsenic thiolate complexes. *Inorg. Chem.*, **44**, 9634–9636.
60. Starbuck, J., N. C. Norman, and A. G. Orpen, 1999. Secondary bonding as a potential design element for crystal engineering. *New J. Chem.*, **23**, 969–972.
61. Bondi, A. 1964. Van der waals volumes and radii. *J. Phys. Chem.* **68**, 441–451.
62. Allen, F. H., J. E. Davies, J. J. Galloy, O. Johnson, O. Kennard, C. F. Macrae, E. M. Mitchell, G. F. Mitchell, J. M. Smith, and D. G. Watson, 1991. The development of version-3 and version-4 of the Cambridge Structural Database system. *J. Chem. Inf. Comput. Sci.*, **31**, 187–204.
63. Allen, F. H. and O. Kennard, 1993. *Chem. Des. Autom. News*, **8**, 31–37.
64. Changes in the absorption spectrum of an aromatic system due to interactions between a phenyl ring and the lone pair of a nearby oxygen moiety have

been reported: Rao, C. N. R. 1975. *Ultra-violet and Visible Spectroscopy*, 3 ed., Butterworth & Co. Ltd., London.
65. Perkampus, H. H. 1992. Eda complexes. In *UV-vis Spectroscopy and its Applications*, pp 149–158, Springer-Verlag, New York.
66. Wurthner, F. 2004. Perylene bisimide dyes as versatile building blocks for functional supramolecular architectures. *Chem. Commun.*, 1564–1579.
67. Rademacher, A., S. Markle, and H. L. Langhals, 1982. Losliche perylenfluoreszenzfarbstoffe mit hoher photostabilitat. *Chem. Ber.*, **115**, 2927–2934.
68. Griffin, B. A., S. R. Adams, and R. Y. Tsien, 1998. Specific covalent labeling of recombinant protein molecules inside live cells. *Science*, **281**, 269–272.
69. Johnson, D. W., M. A. Pitt, and J. M. Harris, 2006. Adsorbent with multiple layers U.S. Patent application #11/350,202 (filed feb. 6, 2006).